An Interferometric Interpretation of Marchenko Redatuming

Joost van der Neut, Delft University of Technology; Ivan Vasconcelos, Schlumberger; Kees Wapenaar, Delft University of Technology

Abstract

Recently, an iterative scheme was introduced to retrieve up- and downgoing Green's functions at an arbitrary location F in the subsurface. The scheme uses the reflection data as acquired at the surface as input, together with an estimate of the direct arrival from the surface to location F, which is referred to as the initial focusing function. We interpret the overall action of the scheme as the successive actions of various linear filters, acting on the initial focusing function. These filters involve multidimensional crosscorrelations with the reflection response, time reversals and truncations in time. Inspired by literature on seismic interferometry, we interpret multidimensional crosscorrelation in terms of the subtraction of traveltimes along stationary raypaths. The scheme has been designed for layered media with smooth interfaces. Our interferometric interpretation reveals some of the scheme's limitations when it is applied to more complex configurations. It can be concluded that (downgoing or upgoing) internal multiples that arrive at F with a particular angle can be retrieved only if the initial focusing function (i.e., the direct wave) has visited F with this angle. Consequently, shadow zones that cannot be imaged with primary reflections can theoretically also not be imaged with internal multiples, when the current iterative scheme is used for their retrieval. Finally, we observe that the current scheme does not yet optimally perform in media with point scatterers, since an underlying assumption (generally referred to as the ansatz) is not perfectly obeyed in this case. It is envisioned that this can be improved if truncations in time that are implemented after each iteration are replaced by more-advanced filtering methods.

Introduction

Wapenaar *et al.* (2013) introduced an iterative scheme to retrieve up- and downgoing Green's functions as if there were a receiver at position F in the subsurface and sources at the surface. By deconvolving the retrieved upgoing Green's functions with the retrieved downgoing Green's functions, one can obtain extended images with true amplitudes without artifacts from internal multiples (Vasconcelos and Rickett, 2013). At the core of the scheme, we find the following two relations that we have discretized:

$$\mathbf{g}^{-} = \mathbf{R}\mathbf{f}_1^{+} - \mathbf{f}_1^{-}, \tag{1}$$

$$\mathbf{g}^{+} = -\mathbf{R}\mathbf{Z}\mathbf{f}_1^{-} + \mathbf{Z}\mathbf{f}_1^{+}. \tag{2}$$

In these representations, $\mathbf{g}^{-}$ and $\mathbf{g}^{+}$ are the up- and downgoing Green's functions, respectively, with sources at the surface and receivers at a desired focusing point F. These functions are expressed as vectors with concatenated traces in the time-space domain. Matrix $\mathbf{R}$ involves multidimensional convolution with the reflection response (e.g., the observed data at the surface). Vectors $\mathbf{f}_1^{-}$ and $\mathbf{f}_1^{+}$ are the up- and downgoing constituents of a focusing function. The matrix $\mathbf{Z}$ applies time reversal to any vector by rearranging its elements. With the iterative scheme, we aim to find $\mathbf{f}_1^{-}$ and $\mathbf{f}_1^{+}$. An important observation from the underlying derivation is that $\mathbf{f}_1^{+}$ is, in essence, the inverse of the transmission response of the overburden above F. If this transmission response contains a distinct first arrival, it can be shown that $\mathbf{f}_1^{+} = \mathbf{f}_{1,d}^{+} + \mathbf{f}_{1,m}^{+}$, where $\mathbf{f}_{1,d}^{+}$ contains the time-reversed direct arrival and $\mathbf{f}_{1,m}^{+}$ is a coda that arrives thereafter. It can be reasoned that both $\mathbf{Z}\mathbf{f}_1^{-}$ and $\mathbf{Z}\mathbf{f}_{1,m}^{+}$ contain no information at or after the first arrival (Wapenaar *et al.*, 2013), whereas the Green's functions contain no information before the first arrival. We exploit this observation by designing a muting function that separates the focusing functions from the Green's functions. This muting function is introduced by matrix $\mathbf{M}$ that removes all information at and after the first arrival (defined as the muting time). Due to causality and the previous statements, we find $\mathbf{M}\mathbf{g}^{+} = \mathbf{M}\mathbf{g}^{-} = \mathbf{0}$, $\mathbf{M}\mathbf{f}_1^{-} = \mathbf{f}_1^{-}$, $\mathbf{M}\mathbf{Z}\mathbf{f}_{1,m}^{+} = \mathbf{Z}\mathbf{f}_{1,m}^{+}$ and $\mathbf{M}\mathbf{Z}\mathbf{f}_{1,d}^{+} = \mathbf{0}$. Hence, applying $\mathbf{M}$ to equations 1 and 2 and rewriting the results, yields

$$\mathbf{f}_1^{-} = \mathbf{M}\mathbf{R}\mathbf{f}_{1,d}^{+} + \mathbf{M}\mathbf{R}\mathbf{f}_{1,m}^{+}, \tag{3}$$

$$\mathbf{Z}\mathbf{f}_{1,m}^{+} = \mathbf{M}\mathbf{R}\mathbf{Z}\mathbf{f}_1^{-}. \tag{4}$$

We can now iteratively update these expressions to find $\mathbf{f}_1^{-}$ and $\mathbf{f}_{1,m}^{+}$, starting with the time-reversed direct arrival as our initial knowledge. Once this is done, the Green's functions can be retrieved with equations 1 and 2. We refer to this methodology as Marchenko redatuming.

Interferometric interpretation

The Marchenko scheme has been designed for layered media with moderately curved interfaces and for limited source-receiver offsets (Wapenaar *et al.*, 2013). To test how it behaves when these conditions are not obeyed, we demonstrate Marchenko redatuming with a synthetic example in a homogeneous medium with three point scatterers. The configuration is shown in Figure 1a. At the surface, 201 sources and 201 receivers are deployed with 20m spacing. A focus point F is chosen at 1000m depth, below the center of the (source and receiver) arrays. Our aim is to retrieve the scattered upgoing and downgoing Green's functions at F, which are shown for reference in Figures 1b and 1c (obtained by direct modelling).

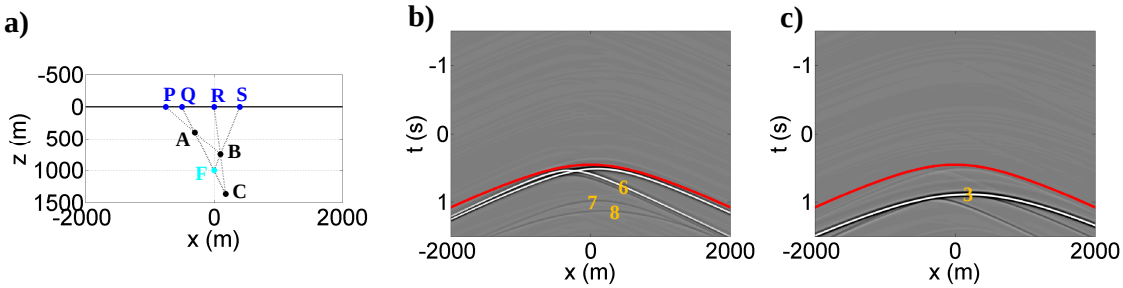

Figure 1: *a) Example with three point scatterers (labeled A, B and C). The black solid line denotes the surface, where sources and receivers are deployed. The cyan dot F denotes the focus point, where we want the Green's functions to be retrieved. The blue dots P, Q, R and S denote stationary points, whereas the dashed lines represent stationary paths. b) The scattered downgoing field and c) the scattered upgoing field with sources at the surface and a single receiver at F. The red curve defines the muting time.*

In the first iteration, the direct field is crosscorrelated (= time-reversed and convolved) with the reflection response. The result of this operation ($\mathbf{Rf}_{1,d}^{+}$) is shown for the fixed focus point F in Figure 2a. Each trace in this gather can be interpreted as a stack over traces in a so-called correlation gather. The correlation gather is the integrand of the multidimensional crosscorrelation that undergirds $\mathbf{Rf}_{1,d}^{+}$, comparable to the correlation gather in seismic interferometry (Schuster, 2009). We show the central trace (shown in cyan in Figure 2a) in Figure 2b. According to equation 3, all information before the muting time (indicated by the red curve in all figures), should be used to update $\mathbf{f}_1^{-}$. As an example, we discuss the retrieval of two events that are labelled as 1 and 2 in the figures. In Figure 2c, we describe their origin by subtracting the traveltimes along stationary raypaths, following similar logic as is common in seismic interferometry (Schuster, 2009). As shown by the diagrams, the events that make up $\mathbf{f}_1^{-}$ contain both causal and acausal legs. Another important observation is that to retrieve these particular events, the stationary points Q and S must be sampled, as can be seen from the cartoons in Figure 2c and from the correlation gather in Figure 2b. Remember that the focusing function is designed such that equation 1 should be satisfied. Therefore, we can find an initial estimate of $\mathbf{g}^{-}$ after the muting time. This is demonstrated by event 3 that can be observed both in Figure 1c (obtained by direct modelling) and in Figure 2a. In Figure 2c, we show that the retrieval of this event stems from backpropagating the primary reflection from scatterer C with the direct field from the surface to F. This is nothing more than conventional inverse wavefield extrapolation. It is important to realise that sampling stationary point Q is essential to do this. It should also be noticed that event 3 is not the only event we can observe after the muting time. As an example, we point to event 4 that is also explained in Figure 2c. This event is generated by interactions of a multiply scattered wave with $\mathbf{f}_{1,d}^{+}$. This is a common type of artefact in conventional inverse wavefield extrapolation, resulting directly from incorrect handling of multiple scattering. We will demonstrate later how this artefact will be eliminated by Marchenko redatuming.

Once $\mathbf{f}_1^{-}$ has been updated with equation 3, we can compute $\mathbf{RZf}_1^{-}$ as it appears in equation 4. In Figures 3a, 3b and 3c, we show the retrieved gather, a correlation gather and the interpretation of four events that are discussed below. We start with event 5, which contains causal and acausal legs. Since it occurs before the muting time, it will be used to update $\mathbf{Zf}_{1,m}^{+}$, following equation 4. Later we show how this event can help us in eliminating artefacts. We also find three events (6-8) after the muting time. In Figure 3c we show that these events are all physical and downgoing at F. This is not surprising, since the focusing function is designed to satisfy equation 2. Hence, we expect to find the

(polarity-reversed) downgoing Green's function $-\mathbf{g}_1^+$ below the muting time. In Figure 1b (obtained by direct modelling), we find indeed the same events 6-8 with reversed polarity.

In the next iteration, we update our estimate of $\mathbf{f}_1^-$ with equation 3. For this, we require the evaluation of $\mathbf{Rf}_{1,m}^+$, see Figure 4. Before the muting time, we find event 9. This event is similar to event 2 in Figure 2, but with reversed polarity. Hence, the amplitude of this event is simply updated during this iteration. We would also like to focus our attention to event 10, stemming from the correlation of event 5 (after time reversal) with the reflection response. If we compare this event with event 4 in Figure 2, we observe that they are kinematically identical. However, since they have opposite polarity, both events cancel when the contributions of $\mathbf{Rf}_{1,d}^+$ and $\mathbf{Rf}_{1,m}^+$ are added (as per equation 1). This confirms that the focusing function has been designed effectively, such that artefacts caused by initial inverse wavefield extrapolation with the direct field (e. g. event 4) are eliminated. A similar lesson can be learned from event 11 in Figure 4. This event cancels an artefact in $\mathbf{Rf}_{1,d}^+$ that is marked as event 12 in Figure 2a and explained in the lowest panel of Figure 4c. Once more, it is observed that events 12 and 11 have opposite polarity and cancel each other during summation of $\mathbf{Rf}_{1,d}^+$ and $\mathbf{Rf}_{1,m}^+$.

Conclusion & discussion

We investigated the behaviour of Marchenko redatuming when it is applied beyond its design criteria. Marchenko redatuming can be interpreted as the successive application of various linear operations (such as multidimensional crosscorrelation, time reversal and muting) applied to the initial focusing function. During these operations, various raypaths are added and subtracted to produce a wide pallet of raypaths between the surface and the focusing point F. The last of these raypaths (connecting with F) always originates from the initial focusing function, without exception. As a consequence, we cannot retrieve any raypath that arrives at F with a particular angle, if the direct ray that arrives at F with this angle is not part of the initial focusing function. This has important consequences for "imaging with multiply reflected waves", because it follows that internal multiples (both down- and upgoing) with a particular angle at F can only be retrieved if the direct wave visits F with the same angle. Hence, it is not possible to image shadow zones with the current iterative scheme, given that the shadow zone cannot be imaged with primary reflections under a particular recording geometry. However, within the aperture of the direct arrivals, Marchenko redatuming still retrieves the full downgoing transmission response and upgoing fields. This correct handling of multiple scattering is highly relevant to improve amplitudes and remove artefacts in depth imaging and inversion. As shown by Wapenaar et al. (2014), the current iterative scheme performs relatively well, even below a strongly scattering overburden.

Another observation is that some desired events are cut off by the muting function. We have seen this in particular with event 2 in Figure 2. This seems a consequence of not perfectly fulfilling the assumption that $\mathbf{f}_1^+ = \mathbf{f}_{1,d}^+ + \mathbf{f}_{1,m}^+$, where $\mathbf{f}_{1,m}^+$ should arrives after $\mathbf{f}_{1,d}^+$. This assumption has been derived for media with smoothly curved interfaces and seems to break in case of point scatterers with lateral separation. However, more research is required to investigate this further. On the other hand, the apex of each individual event in the focusing function seems to arrive before the muting time. Hence, it seems worthwhile to replace the muting function with a more sophisticated separation of Green's functions and focusing functions that utilizes this observation. This might well be done in a different domain (e.g. the curvelet domain), where the separation of these events may be more apparent. Here, we may also use different criteria, namely that the concatenation of causal and acausal legs give the focusing functions significantly different move-out characteristics than the Green's functions. A sophisticated discrimination of focusing functions and Green's functions may also be key to extend the scheme to elastodynamic wave propagation, where a clear separation of the focusing functions and Green's functions (containing converted waves in this case) is not achieved in the time-space domain.

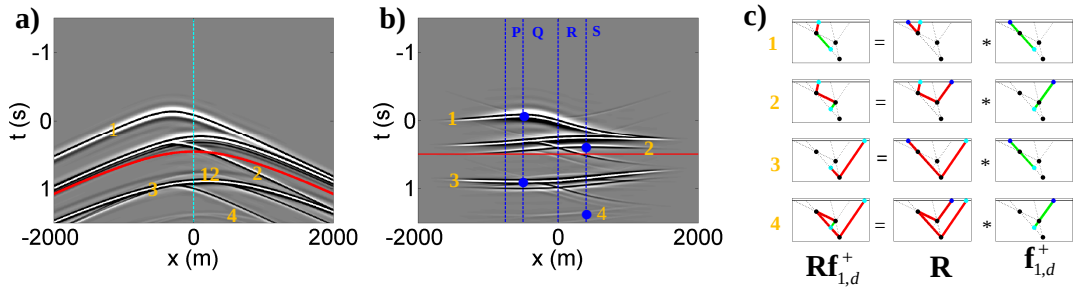

Figure 2: *a) Retrieved gather and b) correlation gather of* $\mathbf{Rf}^{+}_{1,d}$. *The cyan dashed line indicates the trace that is obtained by stacking the traces in Figure 2b. The red curve denotes the muting time. c) Interferometric interpretation of various events. The black dots correspond to the point scatterers, the blue dots indicate stationary points and the cyan dots are arbitrary locations ("end points") at the surface and F. Red rays are causal, green rays are acausal.*

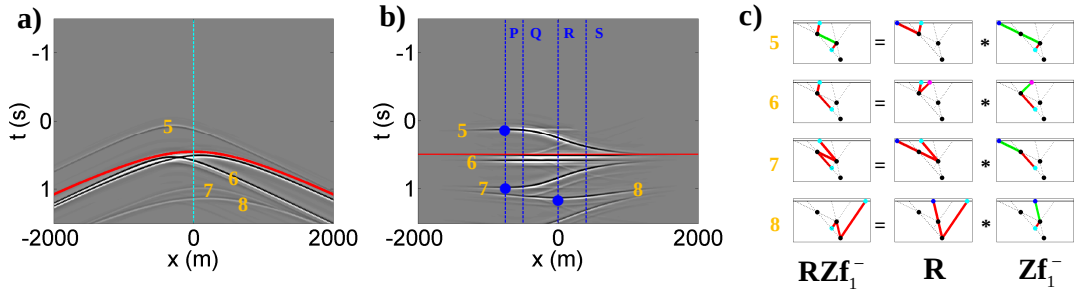

Figure 3: *a) Retrieved gather and b) correlation gather of* $\mathbf{RZf}^{-}_{1}$. *c) Interferometric interpretation of various events. See also the caption of figure 2 for further explanations.*

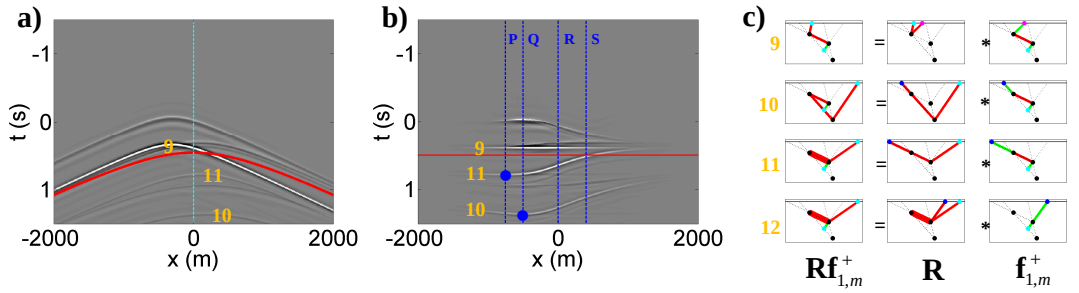

Figure 4: *a) Retrieved gather and b) correlation gather of* $\mathbf{Rf}^{+}_{1,m}$. *c) Interferometric interpretation of various events (for event 12, see Figure 2a). Magenta dots are non-stationary integration locations and the extra-thick raypaths have been evaluated twice (e.g. the event of the reflection response that is correlated to retrieve event 12, scattered first at B, then at A and then at B again). See also the caption of figure 2 for further explanations.*

References

Schuster, 2009, Seismic Interferometry, Cambridge University Press.

Vasconcelos, I. and Rickett, J., 2013, Broadband extended images from joint inversion of multiple blended wavefields, Geophysics, 78, WA147-WA158.

Wapenaar, K., Slob, E., van der Neut, J., Thorbecke, J., Broggini, F. and Snieder, R., 2013, Three-dimensional Marchenko equations for Green's function retrieval "beyond seismic interferometry", 83rd SEG meeting, extended abstracts.

Wapenaar, K., Thorbecke, J., van der Neut, J., Vasconcelos, I. and Slob, E., 2014, Marchenko imaging below an overburden with random scatterers, EAGE Extended Abstracts (This conference).